A marine phytoplankton (Prymnesium parvum) up-regulates ABC transporters and several other proteins to acclimatize with Fe-limitation

著者	Mamunur Rahman M., Azizur Rahman M., Maki Teruya, Nishiuchi Takumi, Asano Tomoya, Hasegawa Hiroshi
journal or publication title	Chemosphere
volume	95
page range	213-219
year	2014-01-01
URL	http://hdl.handle.net/2297/36780

doi: 10.1016/j.chemosphere.2013.09.001

A Marine Phytoplankton (*Prymnesium parvum*) Up-regulates ABC Transporters and Several other Proteins to Acclimatize with Fe-Limitation

M. Mamunur Rahman[1, 2, *]; M. Azizur Rahman[1, 3]; T. Maki[4]; T. Nishiuchi[5]; T. Asano[5] and H. Hasegawa[4, *]

[1]Graduate School of Natural Science and Technology, Kanazawa University, Kakuma, Kanazawa, 920-1192, Japan

[2]Bangladesh Rice Research Institute (BRRI), Gazipur-1701, Dhaka, Bangladesh

[3]Centre for Environmental Sustainability, School of the Environment, University of Technology Sydney, PO Box 123, Broadway, NSW 2007, Australia

[4]Institute of Science and Technology, Kanazawa University, Kakuma, Kanazawa 920-1161, Japan

[5]Division of Functional Genomics, Advanced Science Research Center, Kanazawa University, Takaramachi, Kanazawa, 920-0934, Japan

[*]Corresponding authors

E-mail: rahmanmmamunur@gmail.com (M. Mamunur Rahman)

hhiroshi@t.kanazawa-u.ac.jp (H. Hasegawa)

Tel:/Fax: 81-76-234-4792

Abstract

Iron (Fe) is one of the vital limiting factors for phytoplankton in vast regions of the contemporary oceans, notably the high nutrient low chlorophyll regions. Therefore, it is apparent to be acquainted with the Fe uptake strategy of marine phytoplankton under Fe-limited condition. In the present study, marine phytoplankton *Prymnesium parvum* was grown under Fe-deplete (0.0025 μM) and Fe-rich (0.05 μM) conditions, and proteomic responses of the organism to Fe conditions were compared. In sodium dodecyl sulfate (SDS) gel electrophoresis, 7 proteins (16, 18, 32, 34, 75, 82, and 116 kDa) were highly expressed under Fe-deplete condition, while one protein (23 kDa) was highly expressed under Fe-rich condition. These proteins were subjected to 2-dimensional gel electrophoresis (2-D DIGE) to differentiate individual proteins, and were identified by matrix-assisted laser desorption-ionization-time of flight-mass spectrometer (MALDI-TOF-MS) analysis. The results showed that under Fe-deplete condition *P. parvum* increases the biosynthesis of ATP binding cassette (ABC) transporters, flagellar associated protein (FAP), and Phosphoribosylaminoimidazole-succinocarboxamide synthase. These proteins are assumed to be involved in a number of cellular biochemical processes that facilitate Fe acquisition in phytoplankton. Under Fe-deplete condition, *P. parvum* increases the synthesis of ribulose biphosphate carboxylase (RuBisCo), malate dehydrogenase, and two Fe-independent oxidative stress response proteins, Manganese superoxide dismutase (MnSOD) and Serine threonine kinase (STK). Thus, marine phytoplankton may change their Fe acquisition strategy by altering the biosynthesis of several proteins in order to cope with Fe-limitation.

Keywords: Marine phytoplankton, *Prymnesium parvum,* Iron limitation, protein expression, ABC transporter.

1. Introduction

Marine phytoplankton and cyanobacteria account for half of the global primary production, and they play a major role in regulating global climate by sequestering carbon dioxide from the atmosphere (Benner, 2011). Iron is an important limiting factor for marine phytoplankton and cyanobacteria, and many environmental events, (for example, ocean acidification) may result in Fe limitation to phytoplankton by decreasing dissolved Fe concentration in seawater (Shi et al., 2010).

Iron may also greatly influence the ecology and physiology of phytoplankton in open oceans and upwelling regimes (Coale et al., 1996; Hutchins et al., 1998). The oxidized form of Fe, Fe(III), is sparingly soluble in oxygenated open oceans, and therefore occurs at extremely low concentration (Wells et al., 1995). Marine diatoms and other eukaryotic autotrophs usually acquire Fe as dissolved inorganic species (Maranger et al., 1998), however, low concentration of Fe in seawaters and slow rates of water loss from the cells limit the reaction kinetics of Fe with transport ligands on the surface of phytoplankton (Hudson and Morel, 1993). In addition, sub-nanomolar concentration of dissolved Fe in open oceans confines phytoplankton growth (Price and Morel, 1998). Under Fe-starvation conditions, phytoplankton alter Fe acquisition strategy by up-regulating Fe transport competence (Morel, 1987), by reducing Fe(III) chelates, and even by ingesting insoluble Fe (Maranger et al., 1998; Nodwell and Price, 2001) to meet the cellar Fe requirements. However, it is important to ascertain the biosynthesis of proteins responsible for Fe acquisition in phytoplankton to understand the adaptation strategy of the organism to the Fe-deplete condition. In the present study, proteomic responses of marine phytoplankton *Prymnesium parvum* under Fe-deplete condition were investigated. In addition, proteins that were highly expressed under Fe-deplete condition were identified and characterized to understand their roles in cellular biochemical processes and Fe acquisition mechanisms under Fe-deplete conditions.

2. Materials and Methods

2.1. *Phytoplankton pre-culture and maintenance*

Marine phytoplankton *Prymnesium parvum* was collected from Fukuyama Bay, Hiroshima, Japan. The phytoplankton strain was axenic (axenicity was assessed and monitored by 4′ 6-diamidino-2-phenylindole (DAPI) test).

The axenic phytoplankton strain was pre-cultured for two weeks in 60-mL polycarbonate bottles with artificial seawater containing f/2 nutrient solution (Table 1) without Fe (Lyman and Fleming, 1940; Guillard and Ryther, 1962). Modified f/2 nutrient solution in artificial seawater was sterilized by autoclaving (Sanyo Labo, Model: MLS-3780, Japan). $FeCl_3$ (10 μM) solution (in 1 M HCl) was sterilized separately to avoid Fe contamination. Bottles, tips, and micropipettes used in the test were also sterilized by autoclaving. Sterilization was done at 121 °C for 30 min.

The $FeCl_3$ solution was then mixed with the modified f/2 nutrient solution. Before adding Fe (as $FeCl_3$) to the f/2 sterilized nutrient solution, Fe concentration of the solution was measured following the method of Hasegawa et al. (2004) and was found below 0.001 μM. Therefore, it was assumed that there was limited scope of Fe contamination during the sterilization process. Other chemicals and their sources were carefully selected, and the methods of stock solution preparation of the chemicals were also carefully done to avoid any possible Fe contamination. After sterilization, the materials were placed in a clean bench (SANYO, MCV-710ATS, Japan), and they were kept under ultraviolet ray for 20 min. Since Fe (10 μM as $FeCl_3$ in 1M HCl) was added to the nutrient solution after sterilization, and the phytoplankton were grown in the solution only for about 2 weeks, the possibility of precipitation of added $FeCl_3$ was minimal, and EDTA was not necessarily required.

2.2. Growing phytoplankton in test solutions

A 2 mL pre-culture solution of phytoplankton (2×10^3 mL^{-1} cells of logarithmic growth phase) was inoculated in 1 L of Fe-deplete and Fe-rich f/2 nutrient solution in artificial seawater (Table 1) under laminar air flow condition. Iron concentrations in Fe-deplete and Fe-rich medium were 0.0025 and 0.05 μM, respectively. In order to extract sufficient amount of proteins from the cells, the phytoplankton was cultured in 14 (for Fe-deplete) and 8 (for Fe-rich) one-L volume

polycarbonate bottles in a growth chamber. Light and dark schedule in the growth chamber was 12:12 h with 188 μE m^{-2} S^{-1} light intensity. Temperature in the growth chamber was 20±2 °C.

2.3. Extraction of soluble proteins

After reaching logarithmic growth phase, the phytoplankton growth solution was transferred to a 50-mL centrifuge tube and centrifuged at 1,800 rpm (relative centrifugal force; g = 380) for 10 min at 4 °C. The supernatant was removed and the phytoplankton pellet was washed for two times using 2 mL of 10 mM Tris-HCl (pH 7.2). Then 1.5 mL of 10 mM Tris-HCl was added to the sample to make phytoplankton cell suspension of which 1 mL was transferred to a 1.5-mL micro-tube and was sonicated for 20 seconds using an ultrasonic homogenizer (UH-50, Surface Mount Technology (SMT), Japan) at output 5 under ice-cold condition. The phytoplankton cell suspension was then centrifuged at 15,000 rpm (g = 10,000) for 10 min at 4 °C. The supernatant was then transferred to centrifugal filter unite (Amicon Ultra-4, MWCO of 5000 Da, Millipore). The proteins were recovered on the filters after being concentrated by centrifugation at 3,000 rpm (g = 1,000) for 90 min at 4 °C. Protein quantification was performed by the Bradford assay (Bio-Rad, Hercules, CA, USA) (Bradford, 1976). The protein samples were then made equal concentration and were subjected to further analysis.

2.4. Sodium dodecyl sulfate (SDS) gel electrophoresis

After adding 3.75 μL of 20% Triton X-100 [$C_{14}H_{22}O(C_2H_4O)_n$] and 3.75 μL of 50 mM $MgCl_2$ to 30 μL of protein sample of Fe-deplete and Fe-rich treatments, the samples were incubated in ice for 60 min. Equal volume (37 μL) of the sample and buffer solution (125 mM Tris-HCl, 4% sodium dodecyl sulfate (SDS), 10% 2-mercaptoethanol, 10% sucrose, 0.004% bromophenol blue (BPB), pH 6.8) were then mixed together and then incubated for 3 min at 95 °C. A molecular weight marker (MWM) was diluted by 20-times and an equal volume (30 μL) of MWM and buffer were mixed together and then incubated for 3 min at 95 °C. A 20 μL protein sample and MWM were loaded in

14% polyacrylamide gel. The gel was then run in a mini pageRun system (AE-6531, ATTO bioscience & Biotechnology, Japan) for 100 min at 40 mA current using buffer solution prepared with 25 mM Tris-HCl, 0.1% SDS, 192 mM glycine. After electrophoresis, the gel was stained by shaking for 60 min in coomassie brilliant blue (CBB) solution (0.25% CBB R-250, 5% methanol, 7.5% acetic acid). The stained gel was then shaken with de-staining solution (25% methanol, 7.5% acetic acid) until the background color was removed and protein bands were clearly visible. The molecular weights of protein bands were then measured by Alpha-Ease FC (v 4.0) software. Relative abundance of the protein bands from three replications were measured using ImageJ software (US National Institutes of Health). The relative abundance ratio of differentially expressed proteins was statistically analyzed to determine significant differences between their expression levels by Student's *t*-test using SPSS (v17 for windows). A *p*-value of ≤ 0.05 was considered statistically significant.

2.5. Two-dimensional gel electrophoresis (2-D DIGE)

A 50 µL Trichloroacetic acid was mixed with 950 µL of protein sample of each treatment, and was centrifuged at 14,000 rpm (g = 10,000) for 15 min at 4 °C. The supernatant was removed and pellet was dried after washing 3 times with acetone. A 400 µL swelling buffer (urea 7.0 M, thiourea 2.0 M urea, 4% CHAPS, 0.5% IPG buffer, 0.2% DTT, 0.002% BPB) was mixed with the samples and was centrifuged at 14,000 rpm (g = 10,000) for 15 min at 4 °C. Then protein concentrations in the samples were measured using RC DC Protein Assay Kit (Bio-Rad, USA). Approximately 50 µg of protein of each treatment was labeled by using CyDye (Cy3 and Cy5) DIGE Fluors (GE Healthcare, Tokyo, Japan), and was applied on an IPG strip (pH 3-10) in-gel rehydration protocol (Asano et al., 2012). Protein extracts were applied to the IPG dry strips pH 3-10 (18 cm, GE Healthcare, Tokyo, Japan) during the rehydration step followed by focusing for increasing of voltage linearly from 300 to 3,500 V during 1.5 h, followed by additional 5 h at 3,500 V using an IPGphor (GE Healthcare, Tokyo, Japan). After IEF, the IPG strips were equilibrated at room temperature (22±2 °C) for 15 min in an equilibration buffer (50 mM Tris-HCl, pH 8.8, 6.0 M urea,

30% v/v glycerol, 2% w/v SDS, 1% DTT and 0.002% BPB) followed by 15 min in an equilibration buffer containing 25 mg mL^{-1} of iodoacetamide. SDS-PAGE in the second dimension was carried out, using 12% polyacrylamide gel. After electrophoresis, fluorescent signals were detected by a variable Typhoon™ 9400 imager (GE healthcare, Tokyo, Japan). The 2-D gel images were analyzed with the PDQuest Advanced software (Bio-Rad, CA, USA) (Asano and Nishiuchi, 2011). A 0.5 mg protein sample was used for identification purpose. Automated spot detection and matching was applied, followed by a manual spot editing to achieve a sufficient correlation between the gels. An analysis set was created to find the spots with a minimum of around 2-fold increase or decrease between the two replicates of the Fe-deplete and Fe-rich treatments. Only spots that differed significantly ($p < 0.05$) in abundance according to the Student's *t*-test were further investigated for the identification of the proteins.

2.6. Purification and identification of the proteins

The excised spots were subjected to in-gel digestion with trypsin, and the peptides extracted as described elsewhere (Asano and Nishiuchi, 2011). Briefly, excised spots from 2-D gels were washed sequentially by acetonitrile (100%), DTT (10.0 mM) and iodoacetamide (33.0 mM). Then the gels were washed 3 times sequentially by 100 mM NH_4HCO_3 and CH_3CN and then vacuum-dried. A 20 µL trypsin (12.5 ng mL^{-1}) was added to the gels and heated overnight at 37 ℃. The samples were mixed with 200 µL solution of 50% acetonitrile and 5% formic acid. The samples were then evaporated using a centrifuge, and concentrated to a volume of 10-20 µL.

The peptide mixture was analyzed using 4800 plus MALDI-TOF/TOF™ Analyzer (Applied Bioscience, Carlsbad, CA). Samples were prepared for matrix-assisted laser desorption-ionization-time of flight-mass spectrometer (MALDI-TOF-MS) analysis by mixing 1 mL of the peptide sample with 0.5 µL a-cyano-4-hydroxycinnamic acid in 50% acetonitrile/0.1% TFA, and spotting the mixture on a MALDI target (Fernie et al., 2004). For protein identification, MS/MS data were evaluated by considering amino acid substitution and modification against the NCBI database using the Paragon algorithm of ProteinPilot™ v 2.0 software (AB Sciex, California, USA).

3. Results and Discussion

3.1. Growing phytoplankton under Fe-limited media

To demonstrate that one of the culture media was Fe-limited, growth curves were produced after growing the phytoplankton in Fe-rich and Fe-deplete media. The growth of *P. parvum* did not differ for Fe-rich and Fe-deplete growth media up to 8th day. However, the growth of the phytoplankton clearly slowed down and stopped from 9th day for Fe-deplete medium. On the other hand, the phytoplankton showed steady growth up to 15 day for Fe-rich medium (Fig. 1). Slower growth curve for *P. parvum* in Fe-limited media clearly demonstrate that the Fe-deplete medium really was Fe-limited.

3.2. *Protein expression determined by SDS-PAGE*

In SDS gel electrophoresis, seven protein bands of 16, 18, 32, 34, 75, 82 and 114 kDa were highly expressed under Fe-limited condition and one protein band of 23 kDa was highly expressed under Fe-rich condition (Fig. 2a). Relative abundance of the protein bands is presented in Figure 2b which revealed that the phytoplankton *P. parvum* differentially synthesized some proteins of these molecular weights. Biosynthesis of these differentially expressed proteins may help the phytoplankton to change their Fe acquisition strategy under Fe-limited condition to adapt with Fe-limitation.

3.3. *Differentially expressed proteins under Fe-limited condition*

The proteins were also subjected to 2-D DIGE and then analyzed with the PDQuest Advanced software to characterize the differentially expressed proteins. In an iso-electric focusing (IEF) between 3 and 10, 11 spots of significant difference ($p \leq 0.05$) in expression level were identified on the gels. The spots are numbered as shown in Table 2 and in Figure 4. Out of 11 spots, 8 showed an increase while 3 showed a decrease in abundance under Fe-limited condition (Table 2 and Fig. 4).

The differentially expressed proteins were then identified using MALDI-TOF-TOF-MS analysis. However, some spots could not be identified on the gels because they were not well resolved from neighboring spots.

3.4. *Up-regulated proteins under Fe-limited condition*

3.4.1. Proteins that increase Fe uptake

In the present study, 3 proteins (spot ID 1, 4 and 7, Fig. 3) have been found to be highly expressed under Fe-limited condition that may involve in cellular biochemical processes for increasing Fe uptake in the cell. These proteins were identified as - i) flagella-associated protein, ii) Phosphoribosylaminoimidazole-succinocarboxamide synthase, and iii) ABC transporters (Table 2). Although flagella has been reported to play important roles in sensory functions (Rosenbaum et al., 1999; Silflow and Lefebvre, 2001) and in changing swimming direction (Silflow and Lefebvre, 2001) of phytoplankton, the direct involvement of flagella in Fe uptake is unclear. The single-celled green alga *Chlamydomonas reinhardtii* has been reported to have a receptor signal in its flagella, whcih is used for changing swimming direction (Silflow and Lefebvre, 2001). The highly expressed (about 2-fold) flagellar-associated protein (spot ID 7, Fig. 3) in *P. parvum* may help the phytoplankton to locate Fe molecules in the surounding environment under Fe-deplet condition (Fig. 5).

Phosphoribosylaminoimidazole-succinocarboxamide synthase (spot ID 4, Fig. 3) is expressed 3-times higher under Fe-limitated condition than under Fe-rich condition (Table 2). Vriendt et al. (2005) reported that phosphoribosylaminoimidazole-succinocarboxamide synthase is the key enzime for the synthesis of riboflavin, which is necessary for Fe^{+3} reduction (Wells et al., 1995; Worst et al., 1998). Increased biosynthesis of phosphoribosylaminoimidazole-succinocarboxamide synthase in *P. parvum* under Fe-limited condition is assumed to be linked with upregulation of riboflavin synthesis for Fe^{+3} reduction for efficient Fe uptake (Fig. 5). ABC transporter proteins are key membrane-bound proteins for Fe acquisition in phytoplankton (Wells et al., 1995; Hanikenne et

al., 2005). Over 6-fold increase in the abundance of ABC transporters on the gels (spot ID 1, Fig. 3) indicates the direct involvement of this protein in Fe acquisition under Fe-limited condition (Fig. 5).

3.4.2. Proteins involve in photorespiration

Ribuluse biphosphate carboxylase (RuBisCo) large chain protein (spot ID 3, Fig. 3) is expressed about 4-fold higher in *P. parvum* under Fe-limitated condition than under Fe-rich condition (Table 2). Normally, RuBisCo participates in the Calvin cycle (CO_2 fixation) as well as in the oxidative fragmentation of the pentose substrate during the photorespiration process (Garcia et al., 2006). Previous studies have been reported that Fe limitation decreased CO_2 fixation of marine phytoplankton substantially (Davey et al., 2003; Allen et al., 2008). The increased RuBisCo in *P. parvum* in the present study was provably involved in the increase of photorespiration induced by Fe limitation under low CO_2 fixation condition. Allen et al. (2008) also reported increased rate of photorespiration of *P. tricornutum* under Fe limited condition. From the present study, it can be presumed that *P. purvum* increase the biosynthesis of RuBisCo to overcome stresses induced by Fe-limitation.

Photorespiration is a wasteful process and it increases ATP and NADPH requirements (3 ATP and 2 NADPH) for CO_2 fixation, and thylakoid reactions have been thought to satisfy this requirements by producing the ATP and NADPH (Foyer et al., 2009). Findings of the present study suggest that under Fe limited condition phytoplankton produce high amount of ATP synthase (spot ID 2, Fig. 3) for ATP production. The higher abundance of ATP synthase documented here could be, in part, due to the increased photorespiration and ABC transporter use under Fe limitation that has been hypothesized. Increased biosynthesis of malate dehydrogenase under Fe limited condition (spot ID 8, Fig. 3) may also involve in maintaining specific proportion of ATP and NADPH required for photorespiration (Scheibe, 2004). During photorespiration under Fe-limited condition, malate dehydrogenase may also play an important role in directing photosynthetic electrons into the mitochondrial electron transport chain through the Malate:aspartate shuttle system (Fig. 5) (Allen et al., 2008).

3.4.3. Proteins that reduce oxidative stresses

Prymnesium parvum produces about 3-fold higher manganese superoxide dismutase (MnSOD) under Fe-deplete condition compared to Fe-replet condition (spot ID 5, Fig. 3). Peers and Price (2004) also reported the increase of MnSOD production in coastal and oceanic phytoplankton under Fe-limited condition. Marine phytoplankton may produce reactive oxygen species (ROS) through photosynthesis under Fe-limited condition (Oda et al., 1997; Kim et al., 1999; Wolfe-Simon et al., 2005). The ROS include superoxide (O_2^-), hydrogen peroxide (H_2O_2), and hydroxyl radical (Halliwell, 1982). The photorespiratory pathway is assumed to be a major source of H_2O_2 in photosynthetic cells (Allen et al., 2008). Superoxide is highly reactive and destructive because it cannot diffuse across the cell membranes, and therefore, must be destroyed at the site of production (Wolfe-Simon et al., 2006). Superoxide dismutases (SODs) are enzymes of polyphyletic family that protect cells from destructive reaction of superoxides, and phytoplankton appear to rely primarily on MnSOD for SOD (Fig. 5) (Peers and Price, 2004). In the present study, the higher occurrence of MnSOD (about 3-fold) under Fe-limited condition presumably facilitates the rapid destruction of ROS, which is inevitably generated photochemically from the reaction centers in photosystems (Wolfe-Simon et al., 2006) and in photorespiration (Kitayama et al., 1999; Allen et al., 2008).

Serine threonine kinase (STK), an oxidative stress response protein, was up-regulated 2-fold under Fe-limited condition (spot ID 6, Fig. 3) compared to Fe-replete condition (Table 2). The STK production has been reported to be induced by Fe-limitation (Cheng et al., 2006), and a STK gene (*pkn*22) expression has been confirmed in cyanobacteria (Xu et al., 2003; Zhang et al., 2007) under Fe-deficient condition. It is likely that under Fe-limited condition, light-generated electrons in cyanobacteria cells are not sufficiently consumed, and ultimately cause oxidative stress in photosystems (mainly in PSI) (Straus, 1994). The STK may help the micro-organisms to adapt with the oxidative stress condition inactivating the access electrons (Xu et al., 2003).

4. Conclusions

Under Fe-limited condition, marine phytoplankton *P. parvum* alters some of its cellular biochemical processes by up-regulating proteins some of which are assumed to be involved in Fe uptake. *Prymnesium parvum* may increase Fe uptake efficiency by extracellular Fe^{+3} reduction (mediated by phosphoribosylaminoimidazole-succinocarboxamide synthase) and by increasing Fe acquisition sites (mediated by ABC transporters), in particular the ATP synthase alpha subunit, when they are grown under Fe-limited condition. Under Fe-limited condition, RuBisCo is up-regulated due to increased photorespiration, which needs high metabolic energy and was induced by low CO_2 fixation under Fe limitation. The phytoplankton satisfies the demand of high metabolic energy by increasing ATP synthase. Fe-limitation induces oxidative stresses in phytoplankton. *Prymnesium parvum* is assumed to up-regulate oxidative stress response proteins MnSOD and STK to minimize the oxidative stresses by inactivating the access electrons in the cells. However, the occurrences and action sites of up-regulated proteins phytoplankton under Fe-limited condition are to be determined to be acquainted with the detail cellular biochemical mechanisms.

Acknowledgement

This research was financially supported by a Grant-in-Aid (K2319) for scientific research from the Ministry of the Environment, Japan. The authors would like to thank Dr Luigi De Filippis, School of the Environmental, University Technology Sydney (UTS), Australia, for reviewing this manuscript prior to submission. I authors highly appreciate the editor and the anonymous reviewers for their comments and suggestions that improved the quality of the paper substantially.

References:

Allen, A.E., LaRoche, J., Maheswari, U., Lommer, M., Schauer, N., Lopez, P.J., Finazzi, G., Fernie, A.R., Bowler, C., 2008. Whole-cell response of the pennate diatom *Phaeodactylum tricornutum* to iron starvation. Proc. Natl. Acad. Sci. 105, 10438.

Asano, T., Kimura, M., Nishiuchi, T., 2012. The defense response in *Arabidopsis thaliana* against *Fusarium sporotrichioides*. Proteome Sci. 10, 61.

Asano, T., Nishiuchi, T., 2011. Comparative analysis of phosphoprotein expression using 2D-DIGE. Methods Mol. Biol. 744, 225-233.

Benner, R., 2011. Loose ligands and available iron in the ocean. Proc. Natl. Acad. Sci. 108, 893-894.

Bradford, M.M., 1976. A rapid and sensitive method for the quantitation of microgram quantities of protein utilizing the principle of protein-dye binding. Anal. Biochem. 72, 248-254.

Cheng, Y., Li, J.H., Shi, L., Wang, L., Latifi, A., Zhang, C.C., 2006. A pair of iron-responsive genes encoding protein kinases with a Ser/Thr kinase domain and a His kinase domain are regulated by NtcA in the cyanobacterium *Anabaena sp.* strain PCC 7120. J. Bacteriol. 188, 4822-4829.

Coale, K.H., Johnson, K.S., Fitzwater, S.E., Gordon, R.M., Tanner, S., Chavez, F.P., Ferioli, L., Nightingale, P., Cooper, D., Cochlan, W.P., 1996. A massive phytoplankton bloom Induced by an ecosystem-scale iron fertilization experiment in the equatorial Pacific Ocean. Nature 383, 495-501.

Davey, M.S., Suggett, D.J., Geider, R.J., Taylor, A.R., 2003. Phytoplankton plasma membrane redox activity: Effect of iron limitation and interaction with photosynthesis. J. Phycol. 39, 1132-1144.

Fernie, A.R., Carrari, F., Sweetlove, L.J., 2004. Respiratory metabolism: Glycolysis, the TCA cycle and mitochondrial electron transport. Curr. Opin. Plant Biol. 7, 254-261.

Foyer, C.H., Bloom, A.J., Queval, G., Noctor, G., 2009. Photorespiratory metabolism: genes, mutants, energetics, and redox signaling. Annu. Rev. Plant Biol. 60, 455-484.

Garcia, J.S., Gratão, P.L., Azevedo, R.A., Arruda, M.A.Z., 2006. Metal contamination effects on sunflower (*Helianthus annuus* L.) growth and protein expression in leaves during development. J. Agric. Food Chem. 54, 8623-8630.

Guillard, R.R.L., Ryther, J.H., 1962. Studies of Marine Planktonic Diatoms: I. Cyclotella Nana Hustedt, and Detonula Confervacea (Cleve) Gran. Can. J. Microbiol. 8, 229-239.

Halliwell, B., 1982. The toxic effects of oxygen on plant tissues. CRC Press, Florida, USA.

Hanikenne, M., Krämer, U., Demoulin, V., Baurain, D., 2005. A comparative inventory of metal transporters in the green alga *Chlamydomonas reinhardtii* and the red alga *Cyanidioschizon merolae*. Plant Physiol. 137, 428-446.

Hasegawa, H., Maki, T., ASANO, K., Ueda, K., Ueda, K., 2004. Detection of iron (III)-binding ligands originating from marine phytoplankton using cathodic stripping voltammetry. Anal. Sci. 20, 89-93.

Hudson, R.J.M., Morel, F.M.M., 1993. Trace metal transport by marine microorganisms: Implications of metal coordination kinetics. Deep Sea Res. I: Ocean. Res. Pap. 40, 129-150.

Hutchins, D.A., DiTullio, G.R., Zhang, Y., Bruland, K.W., 1998. An iron limitation mosaic in the California upwelling regime. Limnol. Oceanogr. 43, 1037-1054.

Kim, C.S., Lee, S.G., Lee, C.K., Kim, H.G., Jung, J., 1999. Reactive oxygen species as causative agents in the ichthyotoxicity of the red tide dinoflagellate *Cochlodinium polykrikoides*. J. Plankton Res. 21, 2105-2115.

Kitayama, K., Kitayama, M., Osafune, T., Togasaki, R.K., 1999. Subcellular localization of iron and manganese superoxide dismutase in *Chlamydomonas reinhardtii* (Chlorophyceae). J. Phycol. 35, 136-142.

Lyman, J., Fleming, R.H., 1940. Composition of sea water. J. Mar. Res. 3, 134-146.

Maranger, R., Bird, D., Price, N., 1998. Iron acquisition by photosynthetic marine phytoplankton from ingested bacteria. Nature 396, 248-251.

Morel, F.M.M., 1987. Kinetics of nutrient uptake and growth in phytoplankton. J. Phycol. 23, 137-150.

Nodwell, L.M., Price, N.M., 2001. Direct use of inorganic colloidal iron by marine mixotrophic phytoplankton. Limnol. Oceanogr., 765-777.

Oda, T., Nakamura, A., Shikayama, M., Kawano, I., Ishimatsu, A., Muramatsu, T., 1997. Generation of reactive oxygen species by raphidophycean phytoplankton. Biosci. Biotechnol. Biochem. 61, 1658.

Peers, G., Price, N.M., 2004. A role for managanese in superoxide dismutases and growth of iron-deficient diatoms. Limnol. Oceanogr., 1774-1783.

Price, N.M., Morel, F.M.M., 1998. Biological cycling of iron in the ocean. In: Sigel, A., Sigel, H. (Eds.). Iron transport and storage in microorganisms, plants, and animals: Metal ions in biological systems. Marcel Dekker AG, pp. 1-36.

Rosenbaum, J.L., Cole, D.G., Diener, D.R., 1999. Intraflagellar transport: The eyes have it. The J. cell biol. 144, 385-388.

Scheibe, R., 2004. Malate valves to balance cellular energy supply. Physiol. Plant 120, 21-26.

Shi, D., Xu, Y., Hopkinson, B.M., Morel, F.M.M., 2010. Effect of ocean acidification on iron availability to marine phytoplankton. Science 327, 676-679.

Silflow, C.D., Lefebvre, P.A., 2001. Assembly and motility of eukaryotic cilia and flagella. Lessons from *Chlamydomonas reinhardtii*. Plant Physiol. 127, 1500-1507.

Straus, N.A., 1994. Iron deprivation: Physiology and gene regulation. In: Bryant, D.A. (Ed.). The molecular biology of cyanobacteria. Kluwer Academic Publishers, The Netherlands, pp. 731-750.

Vriendt, D.K., Theunissen, S., Carpentier, W., De Smet, L., Devreese, B., Van Beeumen, J., 2005. Proteomics of *Shewanella oneidensis* MR-1 biofilm reveals differentially expressed proteins, including AggA and RibB. Proteomics 5, 1308-1316.

Wells, M.L., Price, N.M., Bruland, K.W., 1995. Iron chemistry in seawater and its relationship to phytoplankton: A workshop report. Mar. Chem. 48, 157-182.

Wolfe-Simon, F., Grzebyk, D., Schofield, O., Falkowski, P.G., 2005. The role and evolution of superoxide dismutases in algae. J. Phycol. 41, 453-465.

Wolfe-Simon, F., Starovoytov, V., Reinfelder, J.R., Schofield, O., Falkowski, P.G., 2006. Localization and role of manganese superoxide dismutase in a marine diatom. Plant Physiol. 142, 1701-1709.

Worst, D.J., Gerrits, M.M., Vandenbroucke-Grauls, C.M.J.E., Kusters, J.G., 1998. Helicobacter pylori ribBA-mediated riboflavin production is involved in iron acquisition. J. Bacteriol. 180, 1473-1479.

Xu, W.L., Jeanjean, R., Liu, Y.D., Zhang, C.C., 2003. *pkn22* (*alr2502*) encoding a putative Ser/Thr kinase in the cyanobacterium *Anabaena sp.* PCC 7120 is induced by both iron starvation and oxidative stress and regulates the expression of *isiA*. FEBS Lett. 553, 179-182.

Yoshida, K., Terashima, I., Noguchi, K., 2007. Up-regulation of mitochondrial alternative oxidase concomitant with chloroplast over-reduction by excess light. Plant Cell Physiol. 48, 606-614.

Zhang, X., Zhao, F., Guan, X., Yang, Y., Liang, C., Qin, S., 2007. Genome-wide survey of putative Serine/Threonine protein kinases in cyanobacteria. BMC Genomics 8, 395.

Table 1: Nutrient concentrations in the f/2 medium in artificial seawater used for growing marine phytoplankton *Prymnesium parvum.*

Nutrient	Concentration (mol)
$NaNO_3$	8.82×10^{-4}
$NaH_2PO_4.2H_2O$	3.85×10^{-5}
$Na_2SiO_3.9H_2O$	3.52×10^{-5}
SeO_2	1.00×10^{-8}
$CoSO_4.7\ H_2O$	4.27×10^{-8}
$ZnSO_4.7\ H_2O$	7.30×10^{-8}
$MnCl_2.4\ H_2O$	9.09×10^{-7}
$CuSO_4.5\ H_2O$	2.80×10^{-8}
$Na_2MO_4.2\ H_2O$	2.89×10^{-8}
$FeCl_3$	*
Vitamine B12	3.69×10^{-10}
Biotin	2.05×10^{-9}
Thiamin HCl	2.97×10^{-7}
HEPES	5.04×10^{-6}

*Iron was not added to the f/2 medium in artificial seawater when it was used for phytoplankton pre-culture. However, Fe concentrations in Fe-rich and Fe-deplete f/2 medium in artificial seawater were 0.0025 and 0.04 μM, respectively.

Table 2: Differentially expressed proteins in *Prymnesium parvum* under Fe-limited (1 to 8) and Fe-rich (9 to 11) conditions identified by MALDI-TOF-MS. The proteins were identified by comparing MS/MS data against the NCBI database using the Paragon algorithm of ProteinPilot.

Spot ID [a]	Protein abundance (Fe-limit/Fe-rich) [b]	Protein's weights (kDa)	pI value	Name of the proteins [c]	Organisms	Acc. no. [d]	Total ProtSore [e]	% Coverage [f]
1↑	0.16	114	4.1	ABC transporter	*Subdoligranulum variabile DSM 15176*	gi|225565920	2.00	7.8
2↑	0.14	82	4.9	ATP synthase alpha subunit, chloroplastic	*Prymnesiophyte C19847*	D9MYI5	2.00	2.6
3↑	0.29	75	4.4	Ribulose bisphosphate carboxylase	*Prymnesium parvum*	Q9GFX2	8.35	21.4
4↑	0.37	32	4.7	Phosphoribosylaminoimidazole-succinocarboxamide synthase	*Sideroxydans lithotrophicus ES-1*	gi|255259484	4.00	7.5
5↑	0.36	16	8.2	Mnaganase superoxide dismutase	*Arabidopsis thaliana*	gi|79313181	1.70	3.5
6↑	0.47	24	4.8	Serine threonine protein kinase	*Paramecium tetraurelia*	gi|145486541	1.52	6.7
7↑	0.53	18	5.6	Flagellar associated protein	*Thalassiosira pseudonana CCMP1335*	gi|224004678	2.68	13.7
8↑	0.60	34	7.1	Malate dehydrogenase	*Thalassiosira pseudonana CCMP1335*	gi|223992865	4.55	10.8
9↓	4.59	23	5.1	Oxygen evolving enhancer 1 precursor	*Isochrysis galbana*	gi|21913169	6.65	41.2
10↓	2.36	23	4.9	Oxygen evolving enhancer 1 precursor	*Isochrysis galbana*	gi|21913169	8.79	44.1
11↓	5.02	23	4.7	Ribose-5-phosphate isomerase	*Phaeodactylum tricornutum CCAP 1055/1*	gi|219120917	6.88	22

[a] Numbers correspond to the 2-D electrophoresis gel in Fig. 2. Proteins up (↑) and down (↓) regulated under Fe-rich and Fe-limit conditions.

[b] Protein abundance was calculated based on the protein concentration/abundance in 2-D gel electrophoresis.

[c] All proteins were identified comparing MS/MS data against the NCBI database using the Paragon algorithm of ProteinPilot.

[d] Accession number in NCBI database.

[e] A measure of evidence of an identified protein calculated from the confidence level of all peptides detected. ProtSore 2 indicates confidence level > 99%.

[f] The percent coverage of all amino acids from a valid peptide matches to the total number of amino acids in the protein.

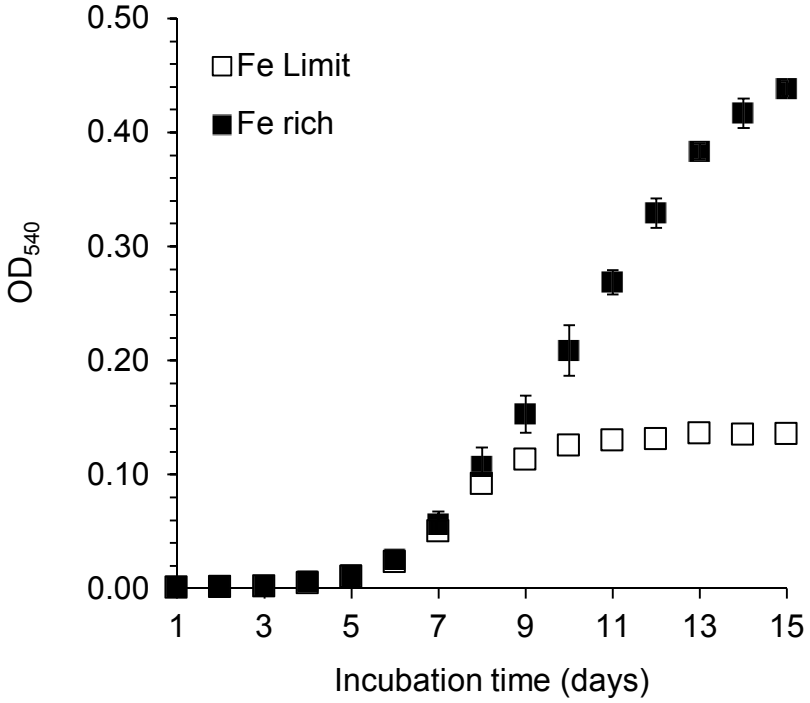

Fig. 1: Growth of marine microalga *Prymnesium parvum* to Fe-limited and Fe-rich conditions. Fe concentrations in Fe-limited and Fe-rich culture medium were 0.0025 and 0.05 μM, respectively. The growth of phytoplankton was calculated based on the optical density at 540 nm wavelength (OD_{540}).

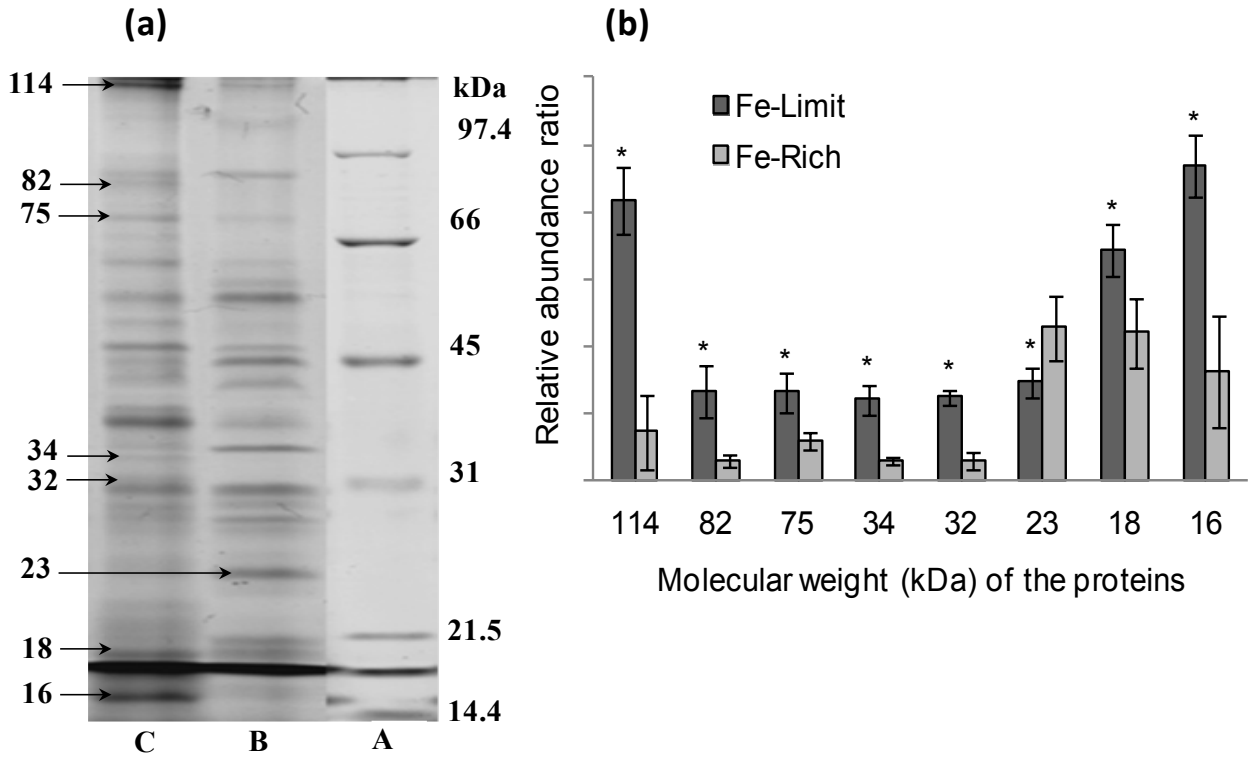

Fig. 2: (a) Protein expression of marine phytoplankton *Prymnesium parvum* in sodium dodecylsulfate polyacrylamide gel electrophoresis (SDS-PAGE) under Fe-rich (Lane B; Fe = 0.05 μM) and Fe-deplete (Lane C; Fe = 0.0025 μM) conditions. Lane A is the molecular marker. Arrows indicate bands of proteins that were up-regulated in Fe-deplete or Fe-rich conditions. **(b)** The band's gray scale intensities were expressed in ratio comparing with average gray scale intensities of gel. Error bars represent standard deviations of three biological replicates. '*' above the bars indicate significant difference ($p \leq 0.05$) according to the Student's *t*-test.

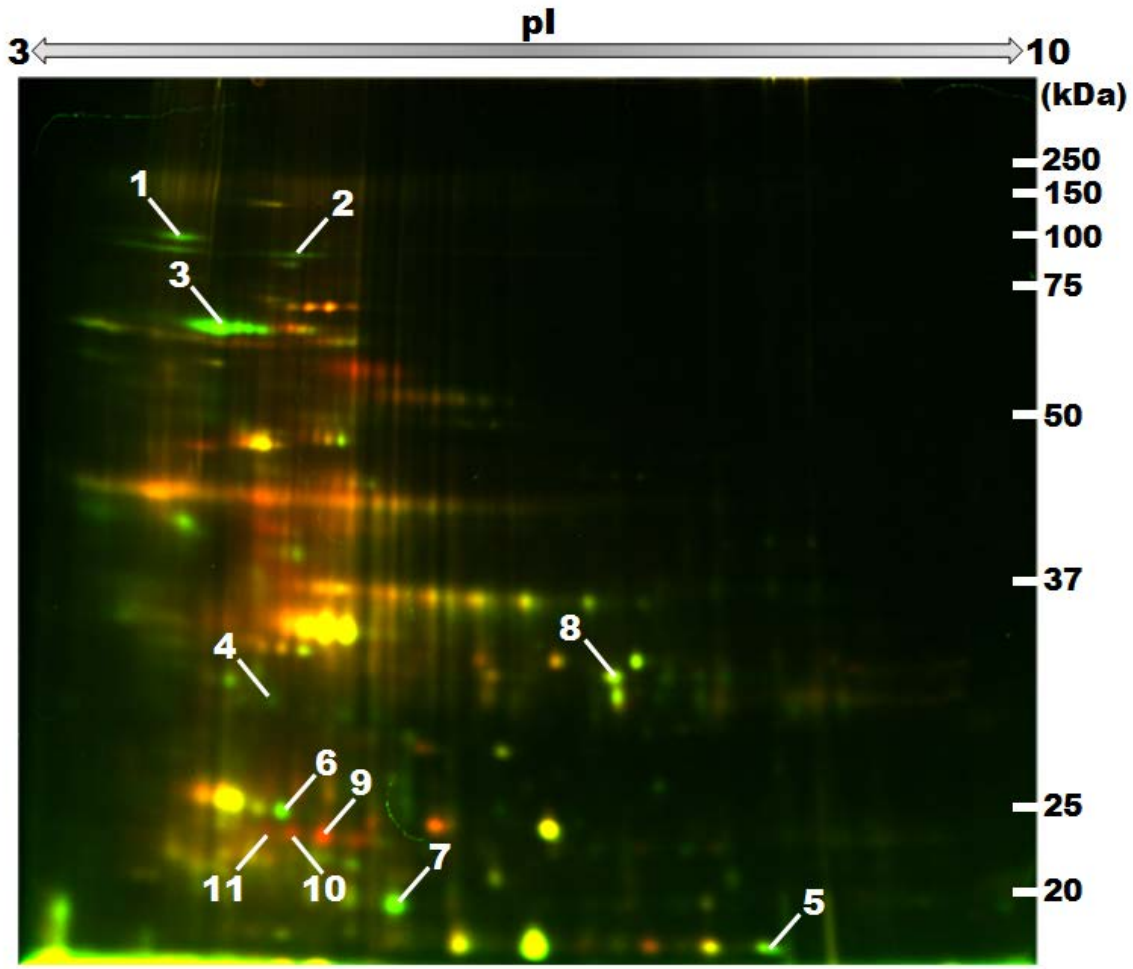

Fig. 3: Two-dimensional differentials in gel electrophoresis (2D-DIGE) analysis of the soluble proteins of marine phytoplankton *Prymnesium parvum* under Fe-rich and Fe-deplete conditions labeled by Cy3 (green) and Cy5 (red), respectively. Selected spots (1 to 10) represent proteins that were differentially expressed under Fe-rich (red) and Fe-deplete (green) conditions.

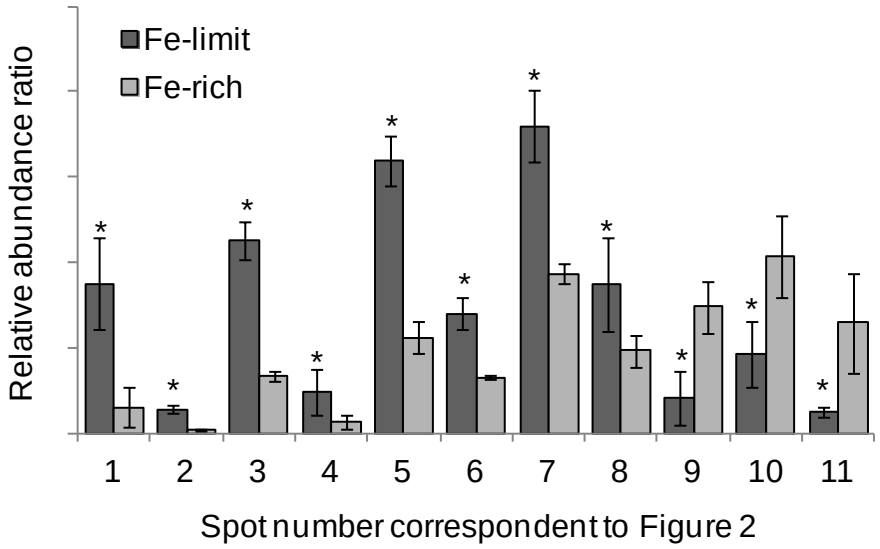

Fig. 4: Graphical representation of relative abundance ratio of differentially expressed proteins in *Prymnesium parvum* under Fe-rich and Fe-limited conditions as separated by two-dimensional differentials in gel electrophoresis (2D-DIGE) analysis. The band's gray scale intensities were expressed in ratio comparing with average gray scale intensities of gel. Error bars represent standard deviations of three biological replicates. '*' above the bars indicate significant difference ($p \leq 0.05$) according to the Student's *t*-test.

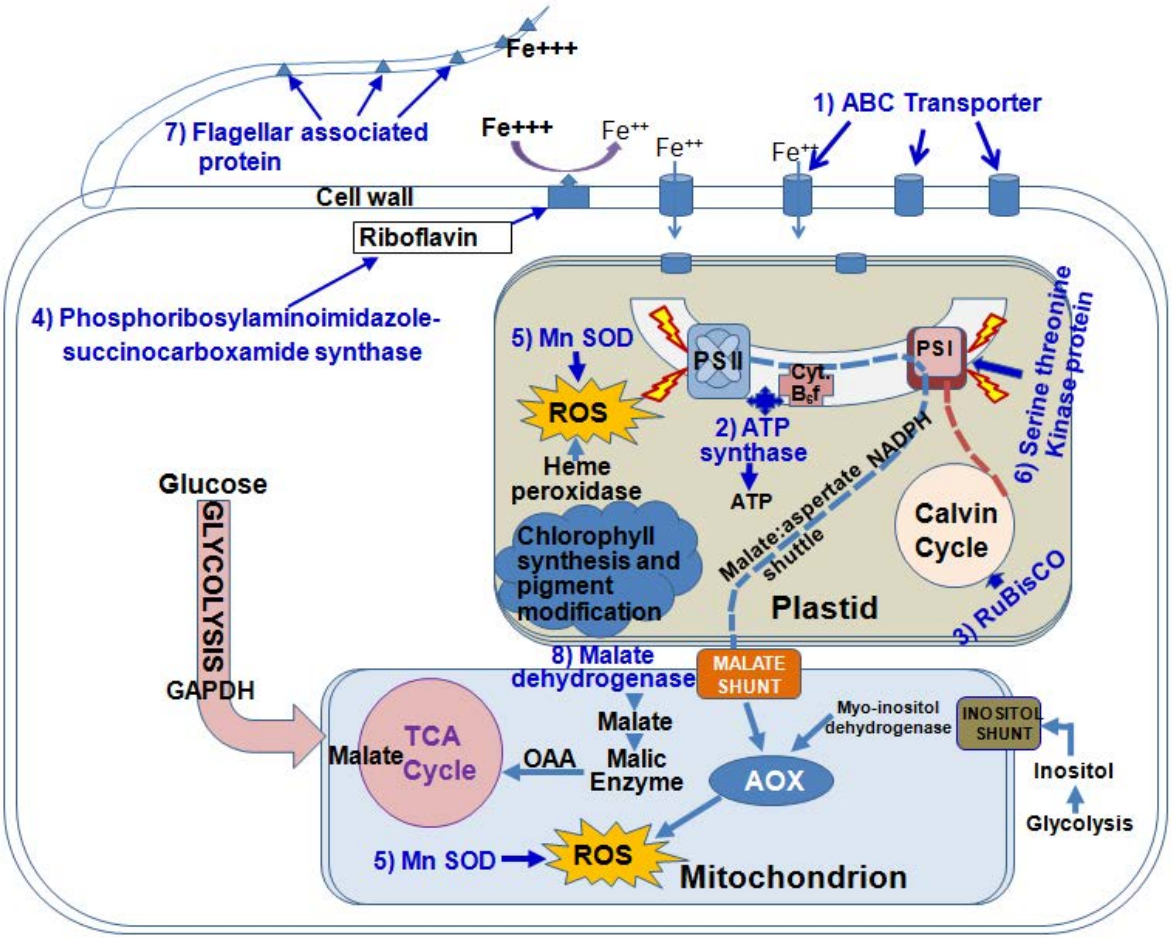

Fig. 5: Biochemical pathways and processes in *Prymnesium parvum* cells under Fe limitation (hypothetical). The figure shows how different proteins (in blue color), up-regulated under Fe-limited conditions, involve in biochemical pathways in *P. parvum* cells. The phytoplankton has two flagella, and the flagellar associated protein (spot ID 7) is provably linked with the flagellar activity of finding iron molecules under Fe-limited condition. Phosphoribosylaminoimidazole-succinocarboxamide synthase (spot ID 4) is associated with the synthesis of riboflavin (Worst et al., 1998), which reduces Fe^{+3} to increase the efficiency of iron uptake in the cell using ABC transporters (spot ID 1). Oxidative stresses induced by photosynthesis (Xu et al., 2003) are supposed to be minimized by Serine threonine kinase protein (spot ID 6). Manganese superoxide dismutase (MnSOD; spot ID 5) may involve in destruction of reactive oxygen species (ROS), which is highly produced in the cells under Fe-limited condition (Wolfe-Simon et al., 2005). RuBisCO takes part in Calvin cycle in photorespiration under Fe-deplete condition (Allen et al., 2008). Under Fe-limited condition, increased malate dehydrogenase (spot ID 8) may help in electron transfer through Malate:aspertale shuttle (Yoshida et al., 2007).